Occurrence of *C*-Glucoside of Resveratrol Oligomers in *Hopea parviflora*

Naohito Abe,[a] Tetsuro Ito,[a] Masayoshi Oyama,[a] Ryuichi Sawa,[b] Yoshikazu Takahashi,[b] Veliah Chelladurai,[c] and Munekazu Iinuma*,[a]

[a] *Laboratory of Pharmacognosy, Gifu Pharmaceutical University; 1–25–4 Daigaku-nishi, Gifu 501–1196, Japan:* [b] *Institute of Microbial Chemistry, Tokyo; 3–14–23 Kamiosaki, Shinagawa-ku, Tokyo 141–0021, Japan: and* [c] *Survey of Medicinal Plant Unit, Central Council for Research in Ayurveda and Siddha; Tirunelveli, Tamil Nadu–627002, India.*
Received September 17, 2010; accepted November 18, 2010; published online November 18, 2010

Investigation of the highly polar chemical constituents in the stem of *Hopea parviflora* (Dipterocarpaceae) resulted in the isolation of four new resveratrol derivatives, hopeasides A and B (1, 2) (resveratrol pentamers), C (3) (resveratrol trimer), and D (4) (resveratrol dimer) together with nine known resveratrol oligomers (5—13). The new structures have a common partial structure of the 1-hydroxy-1-(3,5-dihydroxy-2-*C*-glucopyranosylphenyl)-2-(4-hydroxyphenyl)ethane-2-yl group after oxidative condensation of (*E*)-resveratrol-10-*C*-*β*-glucopyranoside (14). The structures were determined by spectroscopic analysis including 2D-NMR and computer-aided molecular modeling. The biogenetic relationship of the isolates and NMR characteristics caused by steric hindrance are also discussed in this paper.

Key words *Hopea parviflora*; Dipterocarpaceae; resveratrol oligomer; *C*-glucoside; hopeaside

A number of stilbenoids have been isolated from the Dipterocarpaceae family. Our previous phytochemical study demonstrated that the structural diversity is due to the oligomerization degree of the blocking unit of resveratrol, which generates a skeletal variation and complicated stereostructures, and the production of *O*- and *C*-glucosides.[1—14] The genus *Hopea* belongs to Shoreae, one of the two major tribes of the subfamily Dipterocarpoideae, with about 102 species distributed throughout southeast Asia, especially in Indonesia and Malaysia, southern China, southern and eastern India, and Sri Lanka.[15] During this decade, this genus has been well documented to be a good source of biologically active stilbenoids. Stilbenoids have anti-human immunodeficiency virus (HIV),[16] cytotoxic,[17] and acetylcholinesterase inhibitory activities.[18] Although accumulation of our chemical library originated from the other tribe of Dipterocarpoideae, phytochemical aspects of Shoreae, including the genus *Hopea*, have not been comprehensively expanded. Furthermore, our limited studies on *Hopea* (*H. parviflora* in 2000[10] and *H. utilis* in 2001[9]) that deal with a narrow sphere of polarity describing the structure of resveratrol oligomers. In the current study, we focused on the highly polar components present in this tribe and reinvestigated the methanol extract of the stem of *H. parviflora*. This study reports the isolation of four new stilbene glucosides [hopeasides A (**1**)—D (**4**)] along with nine known compounds (**5**—**13**). Their structures were elucidated by extensive spectroscopic methods, including 1D- and 2D-NMR experiments and high-resolution electron spray ionization mass spectra (HR-ESI-MS) analysis, and clarified by computer-aided molecular modeling. The new compounds (**1**—**4**) share a novel substituent, the 1-hydroxy-1-(3,5-dihydroxy-2-*C*-glucopyranosylphenyl)-2-(4-hydroxyphenyl)ethane-2-yl group.

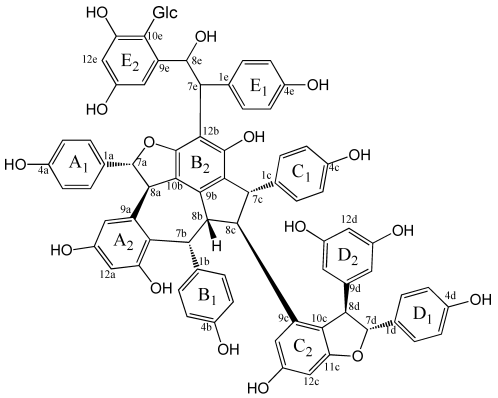

1, **2** *a)*

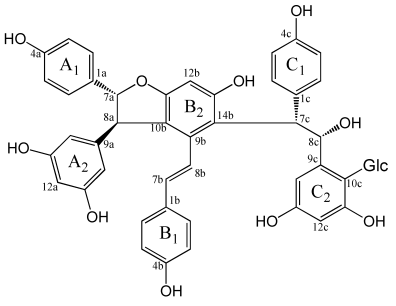

3 *b)*

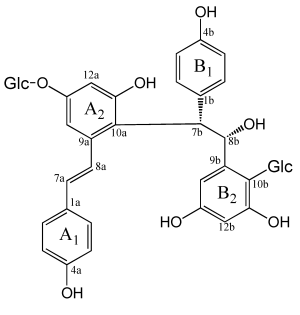

4 *b)*

a) relative structure
b) absolute structure

Results and Discussion

Hopeasides A (**1**) ($[\alpha]_D^{25}$ −8.2°), B (**2**) ($[\alpha]_D^{25}$ +4.8°), C (**3**) ($[\alpha]_D^{25}$ +5.8°), and D (**4**) ($[\alpha]_D^{25}$ +15.5°) were purified from a methanol-soluble fraction of the stem of *H. parviflora* by column chromatography (CC) using stationary phases of silica gel, DMS and Sephadex LH-20, followed by solid

* To whom correspondence should be addressed. e-mail: iinuma@gifu-pu.ac.jp

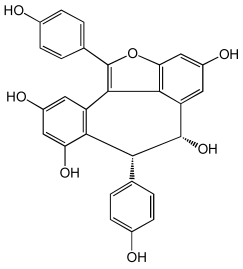

5

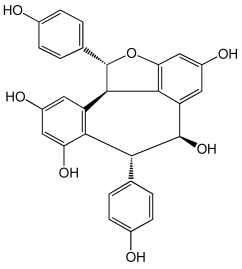

6

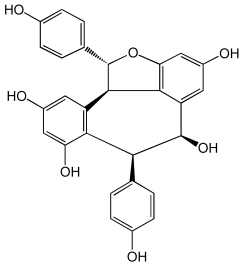

7

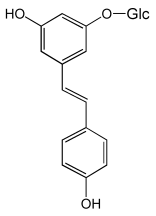

8

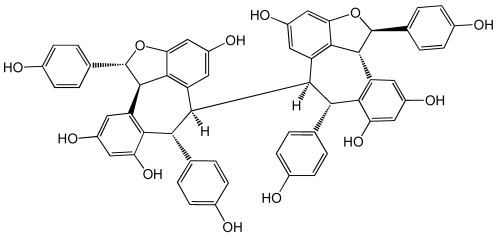

9

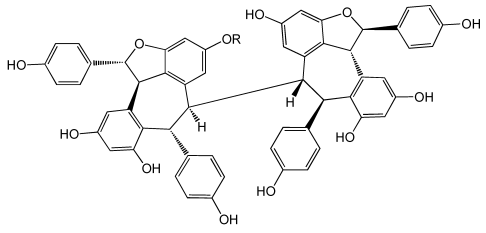

R = H **10**
R = Glc **13**

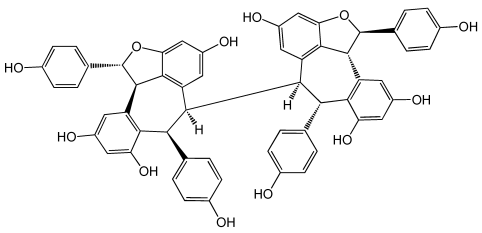

11

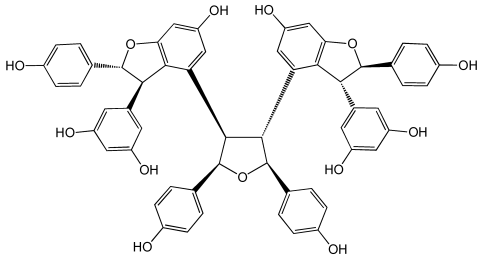

12

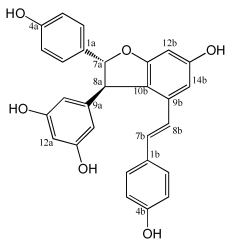

(-)-ε-viniferin

phase extraction with Sep-Pak tC_{18}, and finally preparative HPLC (pHPLC) using stationary phases of octadecyl silica. All compounds gave a positive reaction with the Gibbs reagent.

Stereoisomeric hopeasides A (**1**) and B (**2**) were obtained as a yellowish solid and are the first examples of naturally isolated *C*-glucopyranosyl resveratrol pentamers. The structural analysis for each was similar; hence, the protocol followed for **1** is described in detail. The molecular formula of **1** was confirmed to be $C_{76}H_{64}O_{21}$ from the pseudomolecular ion ($[M+Na]^+$) observed at *m/z* 1335.3846 in positive-mode HR-ESI-MS. ^{1}H- and ^{13}C-NMR spectral data (Table 1) analyzed by double quantum filtered correlation spectroscopy (DQF-COSY), heteronuclear multiple quantum coherence (HMQC) spectra, and heteronuclear multiple bond correlation (HMBC) spectra (Fig. 1, Table 1) showed aromatic signals due to five 4-oxygenated benzene rings (A_1—E_1), three 1,2,3,5-tetrasubstituted benzene rings (A_2, C_2, and E_2), one 3,5-dioxygenated benzene ring (D_2), three mutually coupled aliphatic methine sequences [CH(7a)–CH(8a), CH(7d)–CH(8d), and CH(7e)–CH(8e)], and four aliphatic methine sequences successively coupled in the order [CH(7b)–CH(8b)–CH(8c)–CH(7c)]. Among the methine signals, three protons (H-7a, H-7d, and H-8e) were correlated to the oxygen-substituted carbons [δ_C 90.0 (C-7a), 94.3 (C-7d), and 71.3 (C-8e)] in the HMQC spectrum. After complete assignment of all the quaternary carbons in rings A_1—E_1, A_2, and C_2—E_2, the resorcine-type oxidative pattern of three rings (A_2, C_2, and E_2) were assigned. The remaining six quaternary aromatic carbons (C-9b, C-10b, C-11b, C-12b, C-13b, and C-14b) in the ^{13}C-NMR spectrum (δ_C 140.3, 114.9, 156.8, 112.9, 152.1, and 122.2) were assigned to those of the 3,5-dioxygenated fully substituted benzene ring (B_2). The presence of a *C*-β-glucopyranosyl moiety was supported by NMR spectral data which showed six carbon signals (δ_C 78.6, 73.7, 79.3, 69.9, 80.7, 60.9) and an anomeric proton [δ_H 4.86 (d, J=9.6 Hz)].[4,9,11,13] These results indicated that the aglycone of **1** has the composition $C_{70}H_{52}O_{16}$ corresponding to five Res units (Res A—E; resveratrol A unit: *i.e.*, between rings A_1 and A_2 *via* carbons C-7a and C-8a), which indicated that the aglycone has 44 degrees of unsaturation. The significant ^3J HMBC correlations [H-7a/C-2a(6a), H-8a/C-14a, H-7b/C-2b(6b), H-7c/C-2c(6c), H-8c/C-14c, H-7d/C-2d(6d), H-8d/C-10d(14d), H-7e/C-2e(6e), and H-8e/C-14e] demonstrated the C–C bonds C-1a–C-7a, C-8a–C-9a, C-1b–C-7b, C-1c–C-7c, C-8c–C-9c, C-1d–C-7d, C-8d–C-9d, C-le–C-7e, and C-8e–C-9e, which showed the presence of four Res units (Res A, C—E) and a phenyl ethane moiety (ring B_1–C-7b–C-8b). Further HMBC correlations (H-7b/H-

Table 1. NMR Spectral Data of **1**

No.	δ_H	δ_C	HMBC	NOESY
1a		130.8		
2a (6a)	7.19 (d, 8.4)	130.1	4a, 6a (2a), 7a	7a, 8a, 14a
3a (5a)	6.76 (d, 8.4)	116.0	1a, 4a, 5a (3a)	
4a		158.4		
7a	5.77 (d, 12.0)	90.0	1a, 2a (6a), 9a	2a (6a), 14a
8a	4.30 (d, 12.0)	49.1	1a, 7a, 9a, 10a, 11a,[b] 14a	2a (6a), 2b (6b)
9a		141.6		
10a		125.0		
11a		155.5		
12a	6.34 (d, 2.0)	101.6	10a, 11a, 13a, 14a	
13a		156.6[a]		
14a	6.07 (br s)	106.0	8a, 10a, 12a, 13a	2a (6a), 7a
1b		133.4		
2b (6b)	6.83 (d, 8.8)	130.7	4b, 6b(2b), 7b	7a, 7b, 8c
3b (5b)	6.44 (d, 8.8)	115.7	1b, 4b, 5b(3b)	
4b		155.4		
7b	5.21 (d, 3.2)	37.3	9a, 10a, 11b, 1b, 2b(6b), 8b, 9b	2b(6b)
8b	3.29 (br d, 11.6)	55.2	9b, 14b	7c, 14c
9b		140.3		
10b		114.9		
11b		156.8		
12b		112.9		
13b		152.1		
14b		122.2		
1c		132.3		
2c (6c)	6.68 (d, 8.8)	129.2	4c, 6c (2c), 7c	7c, 8c
3c (5c)	6.51 (d, 8.8)	116.5	1c, 4c, 5c (3c)	
4c		156.6[a]		
7c	4.45 (d, 10.8)	54.2	13b,[b] 14b, 1c, 2c(6c), 8c, 9c	8b, 2c (6c), 14c
8c	3.74 (dd, 11.6, 10.8)	57.6	9c, 10c, 14c	2b (6b), 2c (6c)
9c		141.0		
10c		123.2		
11c		162.0		
12c	6.20 (d, 2.0)	95.7	10c, 11c, 13c, 14c	
13c		159.3		
14c	6.77 (br s)	105.8	10c, 12c	8b, 7c
1d		134.8		
2d (6d)	7.04 (d, 8.8)	127.9	4d, 6d(2d), 7d	7d, 8d
3d (5d)	6.80 (d, 8.8)	116.0	1d, 4d, 5d(3d)	
4d		57.9		
7d	4.88 (br s)	94.3	10c,[b] 11c, 1d, 2d (6d), 9d	2d (6d), 10d (14d)
8d	3.42 (br s)	55.2	10c, 11c, 9d, 10d (14d)	2d (6d), 10d (14d)
9d		147.9		
10d	5.28 (br s)	106.3	8d, 11d(13d), 12d, 14d (10d)	7d, 8d
11d		158.8		
12d	6.04 (t, 2.4)	102.1	10d(14d), 11d(13d)	
13d		158.8		
14d	5.28 (br s)	106.3	8d, 11d (13d), 12d, 14d (10d)	7d, 8d
1e		133.0		
2e(6e)	7.19 (d, 8.4)	131.7	4e, 6e (2e), 7e	7e, 8e
3e(5e)	6.61 (d, 8.4)	114.9	1e, 4e, 5e (3e)	
4e		156.1		
7e	4.78 (d, 6.8)	47.2	11e, 12e, 13e, 1e, 2e (6e), 8e, 9e	2e(6e), 14e
8e	5.80 (d, 6.8)	71.3	1e, 14e[b]	14e, Glc-1
9e		145.0		
10e		113.7		
11e		158.3		
12e	6.19 (d, 2.4)	103.8	10e, 11e, 13e, 14e	
13e		158.1		
14e	6.45 (br s)	106.5	8e, 10e, 12e, 13e	7e
Glc-1	4.86 (d, 9.6)	78.6	9e, 10e, 11e	8e
Glc-2	3.55 (dd, 9.6, 8.8)	73.7		
Glc-3	3.39 (dd, 9.2, 8.8)	79.3		
Glc-4	3.66 (dd, 9.2, 9.6)	69.9		
Glc-5	3.55 (m)	80.7		
Glc-6	3.79 (m)	60.9		

Values are in ppm (δ_H and δ_C). Measured in acetone-d_6 at 400 MHz (^{1}H-NMR) and 100 MHz (^{13}C-NMR). All protons and carbons were assigned by DQF-COSY, HMQC and HMBC spectra. *a*) Overlapping, *b*) weak correlations.

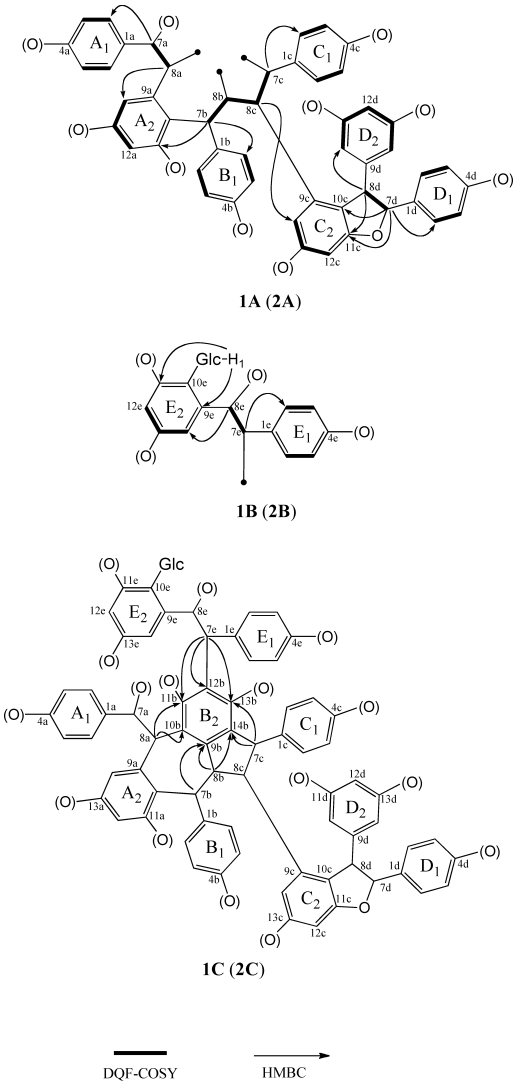

Fig. 1. Selected Correlations in 2D-NMR for the Partial Structures (**1A**—**C**, **2A**—**C**) of **1** and **2**

11a and H-8d/C-11c) supported two single bonds (C-7b–C-10a and C-8d–C-10c). An additional cross-peak observed for H-7d/C-11c supported the presence of an ether linkage, C-7d–O–C-11c, which is part of a dihydrobenzofuran moiety. Long-range correlations between the anomeric proton (δ_H 4.86) and three aromatic carbons (C-9e, C-10e, and C-11e) in the HMBC spectrum confirmed that the *C*-glucopyranosyl group is substituted at C-10e. The 1D- and 2D-NMR spectral evidence showed two connectivities in two partial structures (**1A**, **1B**). The two units are connected through ring B_2, and the C–C linkages (C-8a–C-10b, C-8b–C-9b, C-7c–C-14b, and C-7e–C-12b) were substantiated by the correlations H-8a/C-11b, H-8b/C-14b, H-7c/H-13b, and H-7e/C-11b (**1C**). The connected partial structure (**1C**) has 17 *O*-functions (C-4a, C-7a, C-11a, C-13a, C-4b, C-11b, C-13b, C-4c, C-11c, C-13c, C-4d, C-11d, C-13d, C-4e, C-8e, C-11e, and C-13e) and accounts for 43 of the 44 required degrees of unsaturation for the aglycone ($C_{70}H_{52}O_{16}$), which suggested that the formation of one ring with an ether linkage was necessary. Although no long-range correlation between H-7a/C-11b was observed, the presence of another dihydrobenzofuran moiety (C-7a–C-8a–C-10b–C-11b–O) was deduced after consider-

ing the carbon chemical shifts and the molecular formula of the aglycone. The carbons C-7a, C-8a, and C-9–C-14b in the ^{13}C-NMR spectrum were observed at δ_C 90.0, 49.1, 140.3, 114.9, 156.8, 112.9, 152.1, and 122.2. Similar patterns in the same partial structure were observed in upunoside A (δ_C 89.8, 48.9, 140.4, 116.8, 156.5, 114.0, 151.6, and 121.2) (Fig. 2).[1)] Therefore, the other 16 *O*-functions are OH groups, which consist of 15 phenolics and one aliphatic (C-8e). The ^{1}H-NMR spectrum showed broad signals for one OH group (δ_C 4.50), but the other OH signals of the aglycone were ambiguous in the spectrum. From these data, the planar structure of **1** was confirmed. The aglycone can be regarded as a condensation product of a resveratrol tetramer (**1D**) and a resveratrol monomer (**1E**). The planar structure of **1D** is identical to that of the known resveratrol tetramers hemsleyanols C and D.[11)] In the nuclear Overhauser effect spectroscopy (NOESY) spectrum (Fig. 3), clear cross-peaks between H-2a(6a)/H-8a, H-14a/H-7a, H-2d(6d)/H-8d, and H-10d(14d)/H-7d suggested a *trans* orientation of both dihydrobenzofuran rings (H-7a: β, H-8a: α). Significant nuclear Overhauser effects (NOEs) were observed between H-8a/H-2b(6b), H-2b(6b)/H-8c, and H-8c/H-2c(6c), indicating that H-8a, ring B_1, H-8c, and ring C_1 are situated on the same side of the reference plane (α-orientation). Furthermore, correlations between H-8b/H-7c, H-7c/H-14c, and H-8b/H-14c (weak) supported that H-8b, H-7c, and ring C_2 have β configurations. From these results, the relative configuration of 3,4,4a,5,9b,10-hexahydro-benz[5,6]azuleno[7,8,1-cde]benzofuran was confirmed as [7a(*R*), 8a(*R*), 7b(*R*), 8b(*R*), 7c(*S*), 8c(*S*)]. The configuration of C-7d and C-8d (*R* and *R* or *vice versa*) was determined as follows. Strong NOEs were generally observed between the methine proton and those of the aromatic ring as found for H-7a/H-2a(6a), H-8a/H-14a, and so on. But no NOE was observed for H-8c/H-14c, which indicated that the C–C bond (C-8c–C-9c) is not allowed to freely rotate due to steric hindrance caused by the 3,4,4a,5,9b,10-hexahydro-benz[5,6]azuleno[7,8,1-cde]benzofuran system and 3-(3,5-dihydroxyphenyl)-2,3-dihydro-6-hydroxy-2-(4-hydroxyphenyl)-4-benzofuranyl group, and H-14c is situated on the β-side of the reference plane. A NOESY cross-peak was further observed for H-2d(6d)/H-7b, suggesting that ring D_1 is located near H-7b. Therefore, C-7d and C-8d are determined to have *R* and *R* conifguration. The unit **1D** is the same as hemsleyanol D (**11**). The configuration of **1E** and the relationship between **1D** and **1E** could not be determined by NOESY spectral data because no inter-unit NOEs were observed.

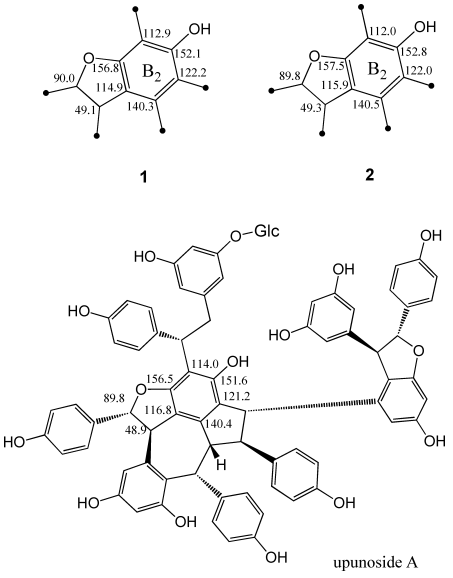

Fig. 2. ^{13}C-NMR Spectral Data of Dihydrobenzofuran Moiety (**1**, **2** and Upunoside A)

The structure of **2** was determined in the same manner as **1**. Analysis of the ^{1}H- and ^{13}C-NMR spectral data by the same protocol on the basis of DQF-COSY, HMQC, and HMBC spectral data (Table 2, Figs. 1, 2) confirmed the partial structures (**2A**, **2B**) and the connection (**2C**), which showed that **2** has the same planar structure as **1**. The ambiguity of ^{1}H- and ^{13}C-NMR signals under certain conditions required various additional conditional NMR measurements. At lower temperature, for example at −20 °C, many aromatic proton signals broaden or disappear, while at higher temperatures give clear signals (data not shown), and hence, we performed detailed NMR spectral analyses at 35 °C and 50 °C. The relative structure of **2** was determined by the results of a

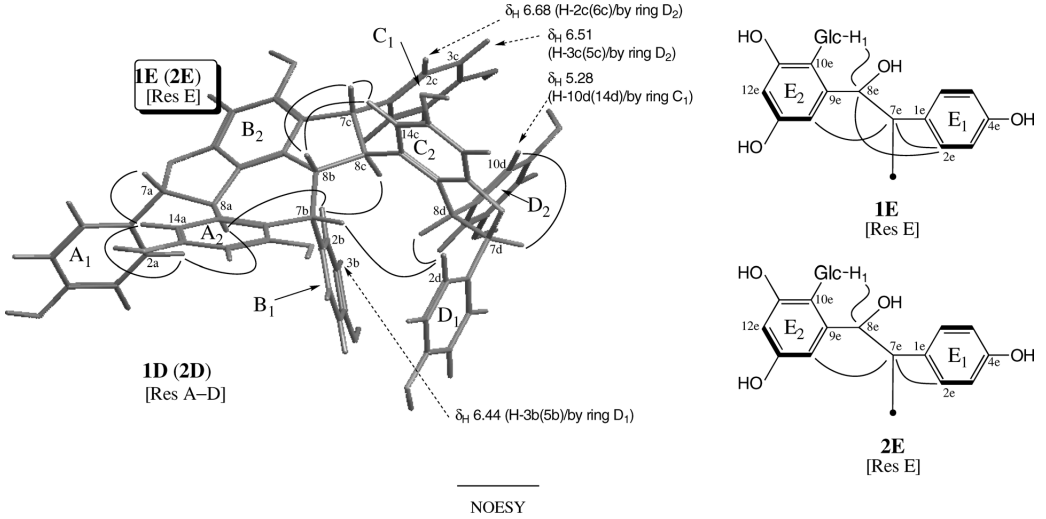

Fig. 3. Selected NOESY Correlations for **1** and **2** and Shielding of Protons by Anisotropy in **1**

The resveratrol tetrameric units (Res A—D) and the monomeric unit (Res E) are represented as **1D** (**2D**) and **1E** (**2E**), respectively.

Table 2. NMR Spectral Data of **2**

No.	35 °C		50 °C			
	δ_H	δ_C	δ_H	δ_C	HMBC	NOESY
1a		131.6*		131.8		
2a (6a)	7.26 (br d)	130.1	7.26 (br d)	130.1	4a, 6a (2a), 7a	8a
3a (5a)	6.82 (d, 8.0)	116.2	6.82 (d, 8.0)	116.2	1a, 5a (3a)	
4a		158.3		158.3		
7a	5.87 (br s)	89.7	5.87 (br d, 12.0)	89.8	2a (6a)	
8a	4.38 (br s)	n.o.	4.38 (d, 12.0)	49.3	1a, 7a, 9a, 10a, 14a, 9b, 10b, 11b	2a (6a), 2b (6b)
9a		142.0		142.1		
10a		125.1		125.2		
11a		155.7[d)]		155.6[j)]		
12a	6.35 (br s)	101.7	6.35 (br s)	101.7	10a, 11a, 13a, 14a	
13a		156.7[e)]		156.7[k)]		
14a	6.18[a)] (br s)	105.9	6.18[i)] (br s)	106.0	8a, 10a, 12a, 13a	
1b		133.6[f)]		133.7		
2b(6b)	6.93 (d, 8.0)	130.9	6.94 (d, 8.0)	131.0	4b, 6b (2b), 7b	8a, 7b, 8c, 2d (6d)
3b(5b)	6.49[b)] (d, 8.0)	115.4	6.51 (d, 8.0)	115.5	1b, 5b (3b)	
4b		155.7[d)]		155.7[j)]		
7b	5.25 (br s)	37.4	5.25 (br s)	37.6	9a, 10a, 11a, 1b, 2b (6b), 8b, 9b	2b (6b), 8d
8b	3.36 (br d, 11.0)	55.4	3.37 (br d, 11.0)	55.5[l)]	1b, 7b,[n)] 9b, 8c[n)]	7c, 14c
9b		140.3*		140.5		
10b		115.9*		116.2		
11b		157.2*		157.5		
12b		113.9*[,g)]		112.0		
13b		152.8*		152.8		
14b		122.0*		122.0		
1c		133.6[f)]		132.8		
2c (6c)	6.75 (d, 8.0)	129.5	6.76 (d, 8.0)	129.6	4c, 6c (2c), 7c	7c, 8c
3c (5c)	6.47 (d, 8.0)	116.4	6.47 (d, 8.0)	116.5	1c, 5c (3c)	
4c		156.7[e)]		156.7[k)]		
7c	4.56 (d, 10.8)	54.4	4.56 (d, 10.8)	54.5	13b, 14b, 1c, 2c (6c), 8c, 9c	8b, 7c, 14c
8c	3.85 (br dd)	57.5	3.85 (br dd)	57.7	7b,[n)] 8b, 7c, 9c, 10c, 14c	2b (6b), 2c (6c)
9c		141.2		141.3		
10c		123.3		123.3		
11c		162.1		162.3		
12c	6.21 (br s)	95.8	6.22 (br s)	95.9	10c, 11c, 13c, 14c	
13c		159.3		159.3		
14c	6.80 (br s)	105.8	6.80 (br s)	105.9	10c, 12c, 13c	8b, 7c
1d		134.9		135.0		
2d (6d)	7.06 (d, 8.0)	128.0	7.06 (d, 8.0)	128.0	4d, 6d (2d), 7d	2b (6b), 7d
3d (5d)	6.81 (d, 8.0)	116.2	6.81 (d, 8.0)	116.2	1d, 5d (3d)	
4d		158.0		158.0[m)]		
7d	4.91 (br s)	94.4	4.92 (br s)	94.5	10c, 11c, 1d, 2d (6d), 9d	2d (6d), 10d (14d)
8d	3.49 (br s)	55.3	3.52 (br s)	55.5[l)]	10c, 1d, 9d, 10d (14d)	7b, 10d (14d)
9d		148.1		148.1		
10d	5.32 (br s)	106.5	5.32 (br s)	106.6	8d, 12d, 14d (10d)	7d, 8d
11d		158.9		158.9		
12d	6.03 (br s)	102.2	6.03 (br s)	102.2	10d (14d), 11d (13d)	
13d		158.9		158.9		
14d	5.32 (br s)	106.5[h)]	5.32 (br s)	106.6	8d, 12d, 10d(14d)	7d, 8d
1e		134.0		134.1		
2e (6e)	7.06 (d, 8.0)	130.8	7.08 (d, 8.0)	130.9	4e, 6e (2e), 7e	7e
3e (5e)	6.49[b)] (d, 8.0)	115.6	6.51 (d, 8.0)	115.7	1e, 5e (3e)	
4e		156.1		156.1		
7e	4.61[c)] (br s)	49.2	4.63 (br d, 9.0)	49.2	11e, 12e, 13e, 1e, 2e (6e), 8e, 9e	2e (6e), 14d
8e	n.o.	71.5	6.15 (br s)	71.3	7e, 9e, 10e, 14e	Glc-1
9e		145.9		145.9		
10e		113.9[g)]		114.0		
11e		158.0[h)]		158.0[m)]		
12e	6.18[a)] (br s)	103.8	6.18[i)] (br s)	103.8	10e, 11e, 13e, 14e	
13e		158.5		158.5		
14e	6.63 (br s)	106.5	6.63 (br s)	106.6	8e, 10e, 12e, 13e	
Glc-1	4.61[c)] (br s)	79.4	4.61 (br d, 10.0)	79.4	9e, 10e, 11e, Glc-2, Glc-3, Glc-5	8e, Glc-5
Glc-2	3.56 (m)	73.7	3.56 (m)	73.7	10e, Glc-3	
Glc-3	3.42 (dd, 9.2, 8.8)	79.4	3.42 (d, 9.2,8.8)	79.4	Glc-2, Glc-4, Glc-5	
Glc-4	3.59 (m)	70.4	3.58 (m)	70.6	Glc-5, Glc-6	
Glc-5	3.08 (br s)	81.5	3.08 (br s)	81.5		Glc-1
Glc-6	3.67 (m)	61.2	3.55, 3.58 (m)	61.4		

Values are in ppm (δ_H and δ_C). Measured in acetone-d_6 at 600 MHz (^{1}H-NMR) and 125 MHz (^{13}C-NMR). All protons and carbons were assigned by DQF-COSY, HMQC, and HMBC spectra. *a*—*m*) Overlapping, *n*) weak correlation, * not observed. Signals were assigned by HMBC correlations.

NOESY experiment (Fig. 3). By the same spectral arguments, **2D** was confirmed to be the same as **1D** (hemsleyanol D). The NMR spectral data for **1D** and **2D** were similar to that of hemsleyanol D except for the disappearance of a signal due to H-12b and the appearance of a signal due to the 1-hydroxy-1-(3,5-dihydroxy-2-*C*-glucopyranosylphenyl)-2-(4-hydroxyphenyl)ethane-2-yl group (**1E**, **2E**). The configuration of **2E** and the relationship between **2D** and **2E** are ambiguous.

The following aspects were obtained from the spectral similarities and differences between **1** and **2**: (1) the coupling constant of H-7e/H-8e for **1** is 6.8 Hz, while that of **2** had a small value; (2) the common NOESY cross-peaks are H-Glc-1/H-8e, H-14e/H-7e, and H-2e(6e)/H-7e, while **1** displayed additional correlation (H-2e(6e)/H-8e); (3) the presence of common NOESY (H-Glc-1/H-8e, H-14e/H-7e) and the absence of NOESY cross-peaks of H-Glc-1/H-7e and H-14e/H-8e for **1** and **2** indicated that the rotations of the C–C bonds (C-7e–C-8e–C-9e) are restricted; and (4) **2** displayed a more shielded proton (H-Glc-5: δ_H 3.08) than that of **1** (H-Glc-5: δ_H 3.55). Four relative configurations (7e*R*, 8e*R*; 7e*R*, 8e*S*; 7e*S*, 8e*S*; 7e*S*, 8e*S*) are possible for **1E** and **2E**, and we have attempted to differentiate these based on theoretical energy-minimized structures that can explain the aspects (1)—(4), but we have not yet reached a conclusion.

Hopeaside C (**3**), a yellowish solid, has the molecular formula $C_{48}H_{44}O_{15}$ as deduced from the HR-ESI-MS ($[M+Na]^+$ *m*/*z* 883.2574), corresponding to a monoglucoside of a resveratrol trimer. The ^{1}H- and ^{13}C-NMR spectral data showed the presence of three 4-hydroxyphenyl groups (rings A_1—C_1), one 3,5-dioxygenated benzene ring (A_2), one 3,5-dioxygenated-1,2,6-trisubstituted benzene ring (B_2), one 3,5-dioxygenated-1,2 -disubstituted benzene ring (C_2), one mutually coupled aliphatic methine [CH(7a)–CH(8a)] on a dihydrobenzofuran ring, one *trans*-coupled olefinic methine [CH(7b)–CH(8b)], and one *C*-glucopyranosyl group (Table

Table 3. NMR Spectral Data of (−)-*ε*-Viniferin and **3**

No.	(−)-*ε*-Viniferin		**3**			
	δ_H	δ_C	δ_H	δ_C	HMBC	NOESY
1a		133.6		133.3		
2a(6a)	7.21 (d, 8.3)	127.7	7.16 (d, 8.8)	127.9	4a, 6a(2a), 7a	7a, 8a, 10a(14a)
3a(5a)	6.84 (d, 8.3)	115.9	6.79 (d, 8.8)	115.8	1a, 4a, 5a(3a)	
4a	8.42 (br s)	159.3		157.8		
7a	5.43 (d, 5.4)	93.7	5.15 (d, 6.3)	93.7	1a, 2a(6a), 8a, 9a, 10b, 11b	2a(6a), 10a(14a)
8a	4.48 (d, 5.4)	56.9	4.43 (d, 6.3)	57.9	1a, 7a, 9a, 10a(14a), 9b, 10b, 11b	2a(6a), 10a(14a)
9a		147.2		145.0		
10a	6.25 (d, 2.0)	106.8	5.89 (d, 2.0)	106.6	8a, 11a(13a), 12a, 14a(10a)	2a(6a), 7a, 8a, 2b(6b), 7b
11a	8.21 (br s)	159.6		158.9		
12a	6.25 (t, 2.0)	101.9	6.05 (t, 2.0)	101.5	10a(14a), 11a(13a)	
13a	8.21 (br s)	159.6		158.9		
14a	6.25 (d, 2.0)	106.8	5.89 (d, 2.0)	106.6	8a, 13a(11a), 12a, 10a(14a)	2a(6a), 7a, 8a, 2b(6b), 7b
1b	129.7		129.5			
2b(6b)	7.18 (d, 8.5)	128.5	6.87 (d, 8.4)	128.2	3b(5b), 4b, 6b(2b), 7b	7b, 8b
3b(5b)	6.74 (d, 8.5)	116.1	6.62 (d, 8.4)	115.6	1b, 4b, 5b(3b)	
4b	8.45 (br s)	157.9		157.4		
7b	6.92 (d, 16.1)	129.8	6.12 (d, 16.4)	134.0	1b, 2b(6b), 9b	10a(14a), 2b(6b)
8b	6.72 (d, 16.1)	123.2	5.78 (d, 16.4)	124.1	1b, 7b, 9b, 10b, 14b	2b(6b), 7c
9b		136.2		139.6		
10b		119.6		118.7		
11b		162.2		160.6		
12b	6.34 (d, 2.0)	96.6	6.27 (s)	98.6	10b, 11b, 13b, 14b	
13b	8.38 (br s)	157.9		158.3		
14b	6.74 (d, 2.0)	104.0		119.3		
1c				133.8		
2c(6c)			7.18 (d, 9.0)	129.4	3c(5c), 4c, 6c(2c), 7c	7c, 8c
3c(5c)			6.66 (d, 9.0)	115.3	1c, 5c(3c), 4c	
4c				155.9		
7c			4.51 (br s)	50.3	9b, 13b, 14b, 1c, 2c(6c), 8c	2c(6c), 14c, Glc-1
8c			6.33 (br s)	72.2	14b	2c(6c), Glc-1
9c				146.3		
10c				113.4		
11c				157.9		
12c			6.20 (d, 2.4)	104.2	10c, 11c, 13c, 14c	
13c				156.3		
14c			6.44 (d, 2.4)	107.1	8c, 10c, 12c, 13c	7c
Glc-1			4.75 (d, 10.0)	78.8[a)]	9c, 10c, 11c	7c, 8c
Glc-2			3.61 (m)	73.8		
Glc-3			3.47 (dd, 9.2, 8.8)	78.8[a)]	Glc-2	
Glc-4			3.66 (m)	69.6		
Glc-5			3.16 (m)	80.9		
Glc-6			3.62 (m)	60.3		

Values are in ppm (δ_H and δ_C) and *J* in Hz. Measured in acetone-d_6 at 400 MHz (^{1}H-NMR) and 100 MHz (^{13}C-NMR). All protons and carbons were assigned by DQF-COSY, HMQC and HMBC spectra. *a*) Overlapping.

3). In the HMBC spectrum, significant correlations between H-2a(6a)/C-7a, H-10a(14a)/H-8a, H-2b(6b)/C-7b, H-8b/C-10b, H-2c(6c)/C-7c, and H-14c/C-8c were found, indicating that the six rings and six methine carbons are connected by six C–C bonds (C-1a–C-7a, C-8a–C-9a, C-1b–C-7b, C-8b–C-9b, C-1c–C-7c, and C-8c–C-9c) and form three Res units. The units are connected through a dihydrobenzofuran ring (C-7a–C-8a–C-10b–C-11b–O) and a C–C bond (C-14b–C-7c), which was also deduced by HMBC correlations (H-7a/C-11b, H-8a/C-11b, H-7c/C-9b, H-7c/C-13b) (Fig. 4). The location of the glycosyl moiety was C-10c as determined by the HMBC cross-peaks between the anomeric proton (H-Glc-1) and aromatic carbons on ring C_2 (C-9c and C-11c). Subsequently, the planar structure was confirmed. In the NOESY spectrum, NOEs were observed between H-2a(6a)/H-8a, H-2a(6a)/H-14a, and H-7a/H-14a, confirming the *trans* orientation of the two methine protons (H-7a and H-8a). The aglycone can be regarded as the condensation product of a resveratrol dimer [**3A**; ε-viniferin[19)]] and a resveratrol monomer (**3B**). The configuration of **3B** and the stereochemical relationship between **3A** and **3B** was determined by NOESY spectral analysis together with consideration of anisotropy. NOE interactions, H-Glc-1/H-7c, H-Glc-1/H-8c, H-7c/H-14c, H-8b/H-7c, and H-8b/H-14c, as well as the absence of NOEs for H-Glc-1/H-2c(6c), H-Glc-1/H-8b, H-7c/H-Glc-1, H-8b/H-2c(6c), and H-8b/H-8c, indicated the following points: (1) the anomeric proton (H-Glc-1) and two methine protons (H-7c and H-8c) face the same side, and the two C–C bonds (C-7c–C-8c–C-9c) are not permitted to freely rotate and (2) configurations of 7c(*S*) and 8c(*S*) relative to C-Glc-1 (*R*) meet all the NOE requirements (Fig. 5). Existence of NOEs for H-7b/H-10a(14a) and H-8b/H-7c and the absence for H-8b/H-10a(14a) and H-7b/H-7c also indicate the fixation of the bond (C-8b–C-9b). These restrictions of bonds explain the following anisotropic effects. The key point for configurational determination of **3A** and **3B** is anisotropy observed in **3A**; the two olefinic protons appear at lower frequency [δ_H 6.12 (H-7b) and 5.78 (H-8b)] than those of ε-viniferin [δ_H 6.92 (H-7b) and 6.72 (H-8b)] (Table 3). The configurations of 7c(*S*) and 8c(*S*) relative to C-Glc-1 (*R*) can explain the shielding effect on H-8b, which is caused by the ring C_2. The anisotropic situation for H-8b is due to the α-fixed orientation of H-8b caused by the fixation of the bond (C-8b–C-9b). The π-system contributing to the shielding of H-7b is ring A_2, which is inevitably situated on the β-side of the reference plane because H-7b is fixed to the β-orientation. The other configurations for C-7c and C-8c as well as C-7a and C-8a are impossible to fit to the results of the NOESY experiment and the shielding location of H-7b and H-8b. When proton chemical shifts of the rings A_2 and B_1 on ε-viniferin unit were compared, **3** displayed highfield shifted protons [δ_H 5.89 {H-10a(14a)} and 6.87 {H-2b(6b)}] compared to those of ε-viniferin [δ_H 6.25 {H-10a(14a)} and 7.18 {H-2b(6b)}]. These shielding effects are explained by anisotropy due to a face-to-face alignment of the rings A_2 and B_1. The other shielded proton in **3** is H-Glc-5 (δ_H 3.16), which can be explained by the anisotropy of ring B_1. Thus, hopeaside C (**3**) was elucidated as 1-{(*1S*,*2S*)-1-hydroxy-2-(4-hydroxyphenyl)-2-{(*2R*,*3R*)-3-(3,5-dihydroxyphenyl)-2,3-dihydro-6-hydroxy-4-[(*1E*)-2-(4-hydroxyphenyl)ethenyl]-2-(4-hydroxyphenyl)benzofuran-5-yl}ethyl}-2-(β-D-glucopyranosyl)benzene-3,5-diol.

Hopeaside D (**4**) was obtained as a yellow amorphous solid. The molecular formula was deduced as $C_{40}H_{44}O_{17}$ from the $[M+Na]^+$ ion at *m*/*z* 819.2476 from HR-ESI-MS, which corresponded to a diglucoside of a resveratrol dimer. The ^{1}H- and ^{13}C-NMR spectral data (Table 4) displayed signals due to two resveratrol units [CH(7a), CH(8a), CH(7b), CH(8b), rings A_1, A_2, B_1, B_2], one *O*-glucopyranosyl group [Glc-1: δ_H 5.06; δ_C 102.7, 74.9, 78.6, 71.2, 78.4, 62.6], and one *C*-glucopyranosyl group [Glc-2: δ_H 4.07; δ_C 79.9, 73.8, 79.6, 69.9, 81.5, 60.8]. Long-range correlations observed in the HMBC spectrum [H-7a/C-2a(6a), H-8a/C-14a, H-7b/C-2b(6b), H-8b/C-14b, H-7b/C-9a, H-7b/C-11a, H-Glc1-1/C-13a, H-Glc2-1/C-11b] (Fig. 6) showed the C–C bonds in the aglycone (C-1a–C-7a, C-8a–C-9a, C-1b–C-7b, C-8b–C-9b, C-7b–C-10a) and positions of the glucopyranosyl(oxy) groups (C-11a and C-10b). The structure can be regarded as a condensation product of two resveratrol monoglucosides, **4A** (piceid) and **4B**. The configuration was determined by NOESY spectral analysis together with consideration of anisotropy (Fig. 7). NOE interactions were observed between H-Glc2-1/H-8b and H-7b/H-14b, while NOEs for H-Glc2-1/H-7b and H-8b/H-14b were absent, indicating the necessity of an *anti*-orientation of two methine protons (H-7b and H-

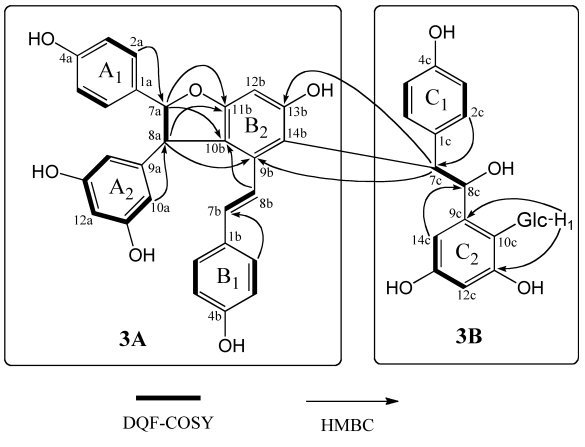

Fig. 4. Selected Correlations in 2D-NMR of **3**

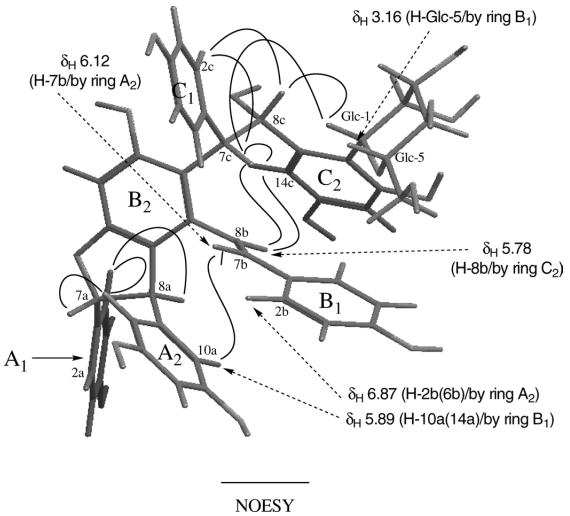

Fig. 5. Stereostructure, Selected NOESY Correlations, and Shielding of Protons by Anisotropy in **3**

Table 4. NMR Spectral Data of **4**

No.	δ_H	δ_C	HMBC	NOESY
1a		130.6		
2a(6a)	7.23 (d, 8.8)	128.9	3a(5a), 4a, 6a(2a), 7a	7a
3a(5a)	6.75 (d, 8.8)	116.6	1a, 2a(6a), 4a, 5a(2a)	
4a		158.5[c]		
7a	6.70 (d, 16.0)	132.5	1a, 2a(6a), 8a, 9a	2a(6a)
8a	7.06 (d, 16.0)	125.8	1a, 9a, 10a, 14a	7b
9a		142.4		
10a		121.0		
11a		158.5[c]		
12a	6.76 (d, 2.4)	103.5	10a, 11a, 13a, 14a	Glc1-1, Glc2-5
13a		157.6[d]		
14a	6.63[a] (d, 2.4)	109.0	8a, 10a, 12a, 13a	Glc1-1
1b		132.5		
2b(6b)	6.89 (d, 8.8)	131.6	3b(5b), 4b, 6b(2b), 7b	7b, 8b
3b(5b)	6.52 (d, 8.8)	115.9	1b, 2b(6b), 4b, 5b(3b)	
4b		156.7		
7b	4.39 (d, 10.0)	57.2	1b, 2b(6b), 8b, 9b, 9b, 9a, 10a, 11a	2b(6b), 14b, 8a, Glc2-1
8b	6.13 (d, 10.0)	71.8	1b, 7b, 9b, 10b, 14b	2b(6b), 14b, Glc2-1
9b		147.5		
10b		115.0		
11b		157.6[d]		
12b	6.16 (d, 2.4)	104.3	10b, 11b, 13b, 14b	
13b		159.2		
14b	6.63[a] (d, 2.4)	106.3	8b, 10b, 12b, 13b	7b, 8b
Glc1-1	5.06 (d, 7.6)	102.7	13b, Glc1-3,[e] Glc1-5[e]	12a, 14a, Glc2-5
Glc1-2	3.72 (dd, 8.4, 8.0)	74.9	Glc1-1, Glc1-3	
Glc1-3	3.54[b] (m)	78.6	Glc1-2, Glc1-4	
Glc1-4	3.54[b] (m)	71.2		
Glc1-5	3.54[b] (m)	78.4		
Glc1-6	4.04 (dd, 12.0, 2.0), 3.83 (dd, 12.0, 5.2)	62.6	Glc1-5	
Glc2-1	4.07 (d, 10.4)	79.9	9b, 10b, 11b, Glc2-2	7a, 8a, Glc2-3, Glc2-5
Glc2-2	3.49 (dd, 10.4,8.8)	73.8	10b, Glc2-3	
Glc2-3	3.33 (dd, 10.4,8.8)	79.6	Glc2-1, Glc2-2, Glc2-4	Glc2-1
Glc2-4	3.54[b] (m)	69.9	Glc2-5, Glc2-6	
Glc2-5	2.87 (br dd, 10.0)	81.5	12b, Glc2-1, Glc1-1	
Glc2-6	3.77 (dd, 12.0, 2.0), 3.65 (dd, 12.0, 2.0)	60.8	Glc2-4, Glc2-5	

Values are in ppm (δ_H and δ_C) and J in Hz. Measured in methanol-d_4 at 400 MHz (^{1}H-NMR) and 100 MHz (^{13}C-NMR). All protons and carbons were assigned by DQF-COSY, HMQC and HMBC spectra. *a*—*d*) Overlapping, *e*) interchangeable.

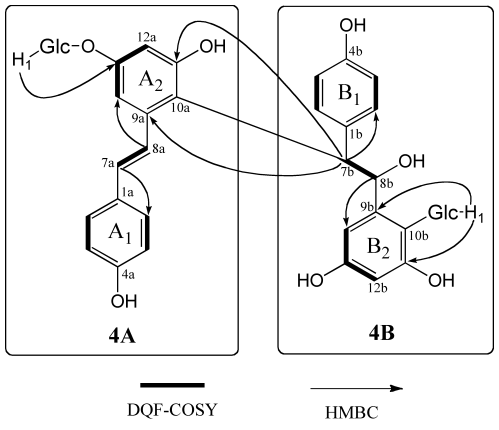

Fig. 6. Selected Correlations Observed in the HMBC Spectrum of **4**

8b). If these are oriented in *syn*, NOE interactions and the following anisotropic evidence would not occur. When the proton chemical shifts due to the *C*-glucopyranosyl units

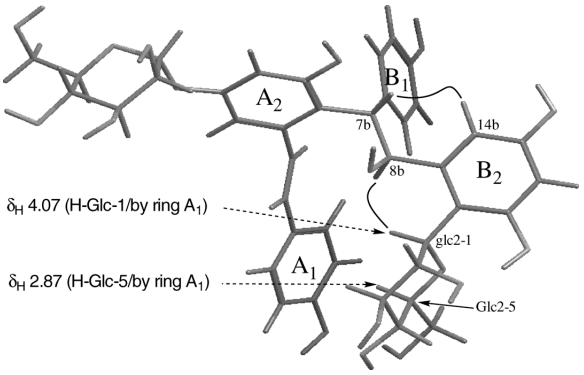

Fig. 7. Stereostructure, Selected NOESY Correlations, and Shielding of Protons by Anisotropy in **4**

were compared, **4** displayed two highfield shifted protons [δ_H 4.07 (H-Glc2-1) and 2.87 (H-Glc2-5)] compared to those of **1**—**3** [**3**: δ_H 4.75 (H-Glc2-1) and 3.16 (H-Glc2-5)]. The cofacial protons (H-Glc-1 and H-Glc-5) are located in the anisotropic region of the ring A_1, which is enabled by the configurations of 7c(*S*) and 8c(*S*) relative to C-Glc-1 (*R*). The other configurations cannot fulfill both NOEs and anisotropy. Thus, hopeaside D (**4**) was elucidated as 1-{(1*S*,2*S*)-1-hydroxy-2-(4-hydroxyphenyl)-2-{1-(β-D-glucopyranosyloxy)-3-hydroxy-5-[(1*E*)-2-(4-hydroxyphenyl)ethenyl]benzene-4-yl}ethyl}-2-(β-D-glucopyranosyl)benzene-3,5-diol.

The new compounds (**1**—**4**) have the common units (**1E**, **2E**, **3B**, **4B**) that may be derived from a blocking unit [10-*C*-glucopyranosyl resveratrol (**14**)]. The occurrence of **14** as a blocking unit in oligostilbenoids is the first instance. Phenolic oxidative coupling of the units (**1D** and **1E**, **2D** and **2E**, **3A** and **3B**, **4A** and **4B**) illustrates plausible biogenetic pathways of **1**—**4** (Chart 1). The explanation for the relationship between the isolates requires the definition of radical precursors. A common radical intermediate is essential when the relationship between the structurally related isolates is considered. The common units for **1**—**4** (**1E**, **2E**, **3B**, **4B**) correspond to the radical (**B**) which would be derived from **14** *via* epoxide (**A**) [Chart 1, (*a*)]. Generation of **1**—**4** by phenolic oxidative coupling is as follows: (1) hopeasides A (**1**) and B (**2**): Hemsleyanol D[11] can be regarded as another precursor of **1** and **2** by consideration of the configurational identity. Radical (**C**) generated from hemsleyanol D would react with **B** and the rearomatization of the resorcinol ring leads to formation of **1** and **2** as the ultimate product [Chart 1, (*b*)]; (2) hopeaside C (**3**): (−)-ε-viniferin (**19**) would generate equilibrium radicals (**D**—**F**), where **D**, **E**, and **F** bear each radical on positions C-12b, C-10b, and C-14b, respectively. Radical (**F**) reacts with **B** to afford **3**. When the reactivities are compared among **D**—**F**, radical **E** is less reactive than **F** due to steric hindrance of the 3,5-dihydroxyphenyl group, **F** is more reactive than **D** because the radical on C-14b can be stabilized by the 4-hydroxyphenylethenyl group, and **F** is more stable than **D** (Chart 1, (*c*)); (3) hopeaside D (**4**): piceid would generate equilibrium radicals (**G**—**I**) in the same way as (−)-ε-viniferin. Radical (**I**), which is more reactive, couples with **B** to form **4**. The lower reactivities of **G** and **H** can be explained by radical instability and neighboring bulky substituents (*O*-glucopyranosyloxy group), respectively (Chart 1, (*d*)).

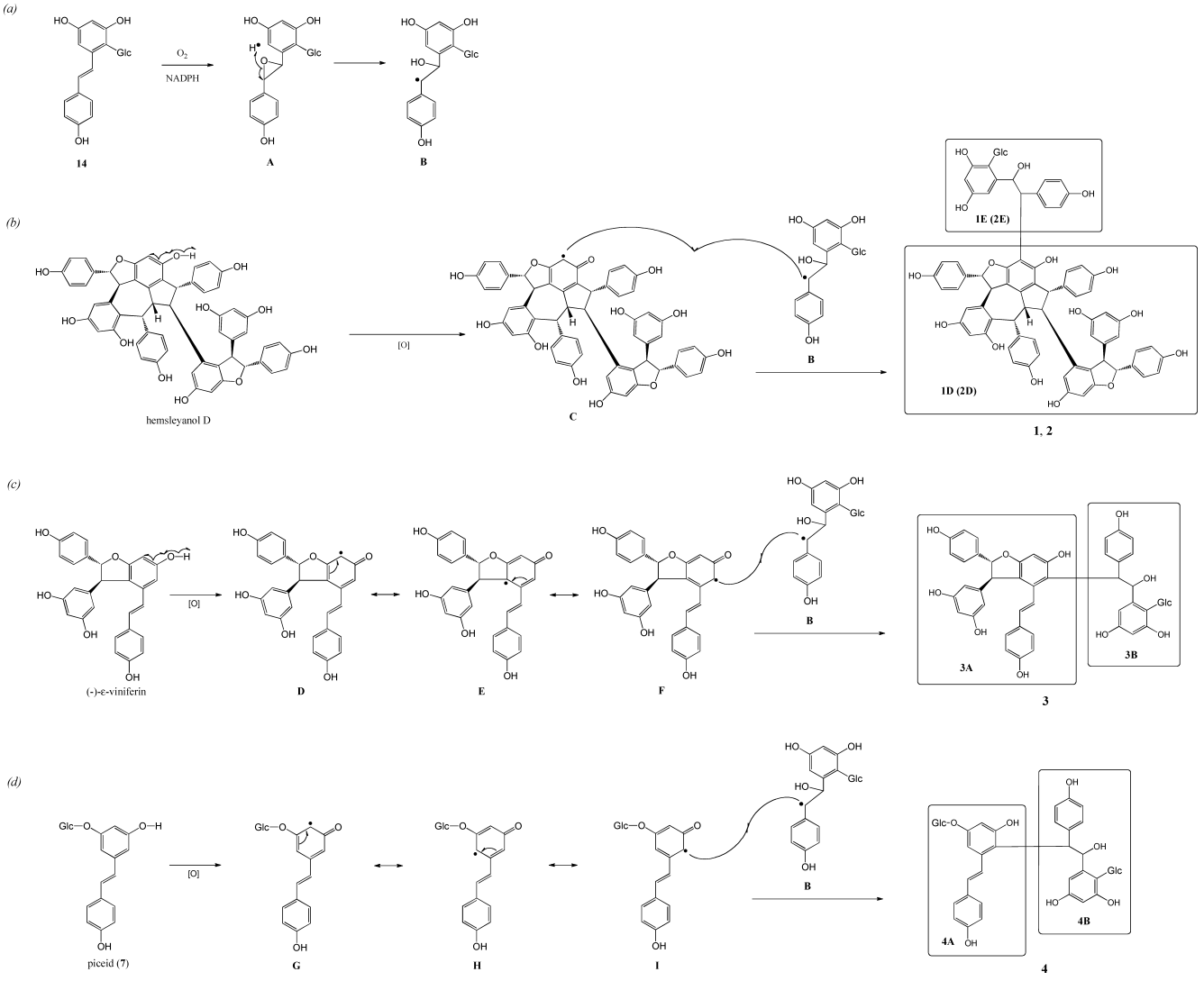

Chart 1. Plausible Biogenetic Pathways of **1**—**4** *via* Intermediates (**A**—**I**)

(*a*) Formation of the common radical intermediate (**B**) *via* epoxide (**A**). (*b*—*d*) Formation of the radical intermediates (**C**, **F**, and **I**) *via* the respective precursors (hemsleyanol D, (−)-*ε*-viniferin, and piceid) and a radical coupling process to give the ultimate products [**1** and **2** (*b*), **3** (*c*), and **4** (*d*)].

In addition to **1**—**4**, nine known compounds were isolated and their structures identified as malibatol (**5**),[16] ampelopsin A (**6**),[10,20,21] balanocarpol (**7**),[21] piceid (**8**), vateriaphenol B (**9**),[6] (−)-hopeaphenol (**10**),[22] pauciflorol C (**11**),[5,14] grandiphenol A (**12**),[14] and vatalbinoside A (**13**)[12] by spectral analysis and comparison with authentic samples.

Experimental

The following instruments were used: optical rotation, Jasco P-1020 polarimeter; CD spectra, Jasco J-820 spectrometer (in MeOH solution); UV spectra, Shimadzu UV-3100 spectrometer; ^{1}H- and ^{13}C-NMR spectra, Jeol JNM-AL-400 spectrometer (chemical shift values are presented as δ values with tetramethylsilane (TMS) as an internal standard); ESI-MS, Jeol-JMS-T100 LC mass spectrometer.

The following adsorbents were used for purification: general analytical TLC, Merck silica gel F_{245} (0.25 mm); column chromatography (CC), Merck silica gel 60 (70—230 mesh), Sephadex LH-20, Fuji Silysia Chemical Chromatorex DMS (100—200 mesh), Waters Sep-Pak Vac 35cc tC_{18} Cartridge, and pHPLC was performed using a Capcell Pak C18 column (UG120, 5 μm, 10 mm i.d.×250 mm, SHISEIDO, Japan) with a Shimadzu 6A pump, Shimadzu SPD-10A UV-VIS detector, and an SPD-M10Avp UV–VIS diode array detector.

The dried bark (1 kg) of *H. parviflora*, collected in India in 1997, was subsequently extracted at room temperature with acetone and methanol (5 l×3 times). The extracts were then concentrated *in vacuo*. The methanol extract was subjected to CC (DMS, MeOH/H_2O of decreasing polarity) to yield fractions A—I. Fr. D (with 20% MeOH; 18.5 g) was fractionated into 12 fractions by CC over silica gel with a mixture of $CHCl_3$–MeOH of increasing polarity. Compounds **5** (21 mg) and **6** (15 mg) were obtained from Fr. D-5 after purification by CC (Sephadex LH-20, MeOH). Purification of Fr. D-8 by repeated CC over Sephadex LH-20 (MeOH) and Sep-Pak tC_{18} (H_2O–MeCN system) achieved the isolation of **3** (42 mg), **7** (24 mg), **8** (51 mg), and **9** (4 mg). Fr. D-8 was further purified by Sephadex LH-20 (MeOH), Sep-Pak tC_{18} (H_2O-MeCN system), and HPLC (H_2O–MeCN system), and yielded **1** (13 mg), **2** (28 mg), **4** (13 mg), **10** (12 mg), **11** (28 mg), **12** (40 mg), and **13** (30 mg).

Hopeaside A (**1**): A yellow solid; $[\alpha]_D^{25}$ −8.2° (c=0.1, MeOH); CD (c=7.62 μM, MeOH) nm ($\Delta\varepsilon$): 215 (+53.7), 242 (−38.3), 270 (−1.2), 283 (−3.4), 297 (+2.6); UV (MeOH) λ_{max} (log ε): 228.2 (5.25), 284.9 (4.58) nm; positive ion ESI-MS m/z: 1335 $[M+Na]^+$; positive ion HR-ESI-MS m/z: 1335.3846 $[M+Na]^+$ (Calcd for $C_{76}H_{64}O_{21}Na$: 1335.3846); ^{1}H-NMR (methanol-d_4, 400 MHz) and ^{13}C-NMR (methanol-d_4, 100 MHz), see Table 1.

Hopeaside B (**2**): A yellow solid; $[\alpha]_D^{25}$ +4.8° (c=0.1, MeOH); CD (c=7.62 μM, MeOH) nm ($\Delta\varepsilon$): 220 (+46.6), 239 (−49.8), 272 (−0.8), 283 (−2.6), 297 (+2.8); UV (MeOH) λ_{max} (log ε): 231.6 (4.77), 283.1 (4.01) nm; positive ion ESI-MS m/z: 1335 $[M+Na]^+$; positive ion HR-ESI-MS

m/z: 1335.3815 $[M+Na]^+$ (Calcd for $C_{76}H_{64}O_{21}Na$: 1335.3832); ^{1}H-NMR (methanol-d_4, 400 MHz) and ^{13}C-NMR (methanol-d_4, 100 MHz), see Table 2.

Hopeaside C (**3**): A yellow solid; $[\alpha]_D^{25}$ +5.8° (c=0.1, MeOH); CD (c=29.1 μM, MeOH) nm ($\Delta\varepsilon$): 208 (−29.1), 222 (+20.9), 237 (−14.8), 250 (+0.7), 285 (−4.3), 303 (+3.4); UV (MeOH) λ_{max} (log ε): 228.2 (5.08), 281.9 (4.40), 317.8 (4.40) nm; positive ion ESI-MS *m/z*: 883 $[M+Na]^+$; positive ion HR-ESI-MS *m/z*: 883.2574 $[M+Na]^+$ (Calcd for $C_{48}H_{44}O_{15}Na$: 883.2572); ^{1}H-NMR (acetone-d_6, 400 MHz) and ^{13}C-NMR (acetone-d_6, 100 MHz), see Table 3.

Hopeaside D (**4**): A yellow solid; $[\alpha]_D^{25}$ +15.5° (c=0.1, MeOH); CD (c=31.4 μM, MeOH) nm ($\Delta\varepsilon$): 212 (−39.1), 219 (−17.8), 231 (−31.2), 250 (+2.2); UV (MeOH) lmax (log ε): 231.2 (4.87), 286.4 (4.62), 323.7 (4.50) nm; positive ion ESI-MS *m/z*: 819 $[M+Na]^+$; positive ion HR-ESI-MS *m/z*: 819.2476 $[M+Na]^+$ (Calcd for $C_{40}H_{44}O_{17}Na$: 819.2471); ^{1}H-NMR (methanol-d_4, 400 MHz) and ^{13}C-NMR (methanol-d_4, 100 MHz), see Table 4.

References

1) Ito T., Ali Z., Iliya I., Furusawa M., Tanaka T., Nakaya K., Takahashi Y., Sawa R., Murata J., Darnaedi D., Iinuma M., *Helv. Chim. Acta*, **88**, 23—34 (2005).
2) Ito T., Furusawa M., Iliya I., Tanaka T., Nakaya K., Sawa R., Kubota Y., Takahashi Y., Riswan S., Iinuma M., *Tetrahedron Lett.*, **46**, 3111—3114 (2005).
3) Ito T., Masuda Y., Abe N., Oyama M., Sawa R., Takahashi Y., Chelladurai V., Iinuma M., *Chem. Pharm. Bull.*, in press, (2010).
4) Ito T., Tanaka T., Ido Y., Nakaya K., Iinuma M., Riswan S., *Chem. Pharm. Bull.*, **48**, 1959—1963 (2000).
5) Ito T., Tanaka T., Iinuma M., Iliya I., Nakaya K., Ali Z., Takahashi Y., Sawa R., Shirataki Y., Murata J., *Tetrahedron*, **59**, 5347—5363 (2003).
6) Ito T., Tanaka T., Iinuma M., Nakaya K., Takahashi Y., Sawa R., Naganawa H., Chelladurai V., *Tetrahedron*, **59**, 1255—1264 (2003).
7) Ito T., Tanaka T., Nakaya K., Iinuma M., Takahashi Y., Naganawa H., Ohyama M., Nakanishi Y., Bastow K. F., Lee K. H., *Tetrahedron Lett.*, **42**, 5909—5912 (2001).
8) Ito T., Tanaka T., Nakaya K., Iinuma M., Takahashi Y., Naganawa H., Ohyama M., Nakanishi Y., Bastow K. F., Lee K. H., *Tetrahedron*, **57**, 7309—7321 (2001).
9) Tanaka T., Ito T., Ido Y., Nakaya K., Iinuma M., Chelladurai V., *Chem. Pharm. Bull.*, **49**, 785—787 (2001).
10) Tanaka T., Ito T., Ido Y., Son T. K., Nakaya K., Iinuma M., Ohyama M., Chelladurai V., *Phytochemistry*, **53**, 1015—1019 (2000).
11) Tanaka T., Ito T., Nakaya K., Iinuma M., Takahashi Y., Naganawa H., Riswan S., *Heterocycles*, **55**, 729—740 (2001).
12) Abe N., Ito T., Ohguchi K., Nasu M., Masuda Y., Oyama M., Nozawa Y., Ito M., Iinuma M., *J. Nat. Prod.*, **73**, 1499—1506 (2010).
13) Ito T., Abe N., Oyama M., Iinuma M., *Tetrahedron Lett.*, **50**, 2516—2520 (2009).
14) Ito T., Tanaka T., Iinuma M., Nakaya K., Takahashi Y., Sawa R., Murata J., Darnaedi D., *Helv. Chim. Acta*, **87**, 479—495 (2004).
15) Ashton P. S., "Flora Malesiana, Ser. I, Spermatophyta," Vol. 9, ed. by Steenis C. G. G. J., Martivus Nijhoff Publishers, Leiden, The Netherlands, 1982, pp. 237—552.
16) Dai J. R., Hallock Y. F., Cardellina J. H. II, Boyd M. R., *J. Nat. Prod.*, **61**, 351—353 (1998).
17) Seo E.-K., Chai H., Constant H. L., Santisuk T., Reutrakul V., Beecher C. W. W., Farnsworth N. R., Cordell G. A., Pezzuto J. M., Kinghorn A. D., *J. Org. Chem.*, **64**, 6976—6983 (1999).
18) Liu J. Y., Ye Y. H., Wang L., Shi D. H. and Tan R. X., *Helv. Chim. Acta*, **88**, 2910—2917 (2005).
19) Sultanbawa M. U. S., Surendrakumar S., Wazeer M. I. M., Bladon P., *J. Chem. Soc., Chem. Commun.*, **1981**, 1204—1206 (1981).
20) Oshima Y., Ueno Y., Hikino H., Ling-Ling Y., Kun-Ying Y., *Tetrahedron*, **46**, 5121—5126 (1990).
21) Diyasena M. N. C., Sotheeswaran S., Surendrakumar S., Balasubramanian S., Bokel M., Kraus W., *J. Chem. Soc., Perkin Trans. I*, **1985**, 1807—1809 (1985).
22) Coggon P., Janes N. F., King F. E., King T. J., Molyneux R. J., Morgan J. W. W., Sellars K., *J. Chem. Soc.*, **1965**, 406—409 (1965).